Hindawi

Research Article

Analysis on the Prewarning Distance of Expressway Traffic Based on Lane-Selection Cell Transmission Model

Yunteng Chen [iD],[1] **Liang Zhao,**[1] **Yong Zhang,**[1] **Jiexin Zhou,**[1] **Liang Yao,**[2] **and Hongwei Lou**[2]

[1]*Shaoxing Communications Investment Group Co., Ltd., Shaoxing, China*
[2]*Alibaba Cloud Computing Co. Ltd., Hangzhou, China*

Correspondence should be addressed to Yunteng Chen; ytchen_traffic@163.com

Lane-changing prewarning is an active management measure used to mitigate the impact of incidents on expressways. This measure affects the operational efficiency and safety of traffic flow upstream of the incident location. To evaluate the effectiveness of this measure in mitigating incident-induced congestion and enhancing traffic safety, it is essential to model and simulate traffic flow on expressways, followed by analyzing the simulation results. In this study, we use the lane-changing selection cell transmission model (ls-CTM) to investigate the impact of setting lane-changing prewarning information on expressway traffic flow. By enhancing the composition of flow within the diverging cell in CTM, traffic can determine its downstream direction based on lane-changing probability rather than the path. A case study was conducted to investigate the impact of prewarning distances of 50, 100, and 150 m on road operational efficiency and traffic safety under different traffic volumes. The effectiveness and applicability of three measures to improve traffic safety were also summarized. The research results can provide more rigorous and effective decision-making support for expressway traffic management and control.

1. Introduction

Traffic incidents often occur on expressways, which not only cause traffic delays but also pose safety threats [1–3]. Therefore, prompt intervention and efficacious safety precautions are imperative. Lane-changing prewarning information is an active measure that can effectively alleviate the impact of incidents [4]. Based on the Intelligent Driver Model, He et al. [4] added lateral lane-changing logic and analyzed the position of lane-changing notifications using traffic simulation software SUMO. Results, which were based on travel time as an efficiency evaluation index, indicated that the effective prewarning distance from the incident point ranged from about 30–300 m under different traffic volumes [4]. However, this study did not fully consider the overall improvement of road section efficiency and safety. To ascertain the impact of the prewarning distance of this measure on mitigating congestion and enhancing traffic safety under incident scenarios, it is necessary to model and simulate the traffic flow on the expressway.

Discrete dynamical models are prevalent forms of traffic flow models for expressway modeling, mainly including cellular automaton (CA) and cell transmission model (CTM). Nagel and Schreckenberg [5] introduced a stochastic discrete automaton model into expressway traffic. Subsequently, researchers have endeavored to improve various types of CA, which are capable of simulating diverse scenarios on expressways. Wang et al. [6] used the CA to study the impact of traffic incidents on the capacity of urban expressways in a mixed-traffic environment. Moreover, some researchers have conducted simulation analysis based on the CA or improved CA models and obtained practical results. Tan et al. [7] simulated a three-lane expressway using the CA and obtained the best speed limit strategy under different traffic conditions by analyzing changes in vehicle travel time, fuel consumption, and emissions under different maximum speed limit strategies.

Although the CA can simulate the behavior of individual vehicles, its simulation may be computationally intensive, especially for large-scale systems, which limits its practical applications. Moreover, it is challenging to calibrate the CA because it requires estimating many parameters that may not

be easy to measure or observe [8]. Compared to microscopic traffic flow models, the CTM only requires fewer computational resources and fewer parameter adjustments to achieve more accurate and comprehensive simulations. Daganzo [9, 10] proposed the CTM after discretizing space-time, which approximates the Lighthill-Whitham-Richards model [11]. Lee [12] extended the CTM framework to encompass interrupted traffic flow modeling. Subsequently, the CTM has found wide-ranging applications in network design [13–15] and network traffic assignment [16–21]. It is noteworthy for its ability to accurately replicate various traffic flow characteristics, as demonstrated in studies [22–24]. In summary, compared to CA, the CTM offers advantages in terms of computational efficiency, and ease of calibration, making it more suitable for large-scale systems and practical applications.

The CTM can be employed to simulate freeways with high degree of precision. Christina et al., integrated a macroscopic lane change prediction model based on cells into the CTM. Experimental results show a negligible difference between the unit occupancy rate of I80 highway data and that of the proposed model [25]. Analyzing freeway traffic flow using the CTM is one of its application directions. Xiao et al. [26] used the CTM to discuss the connectivity probability of Vehicular Ad Hoc Network (VANET) freeway traffic. Wu et al. [27] discovered that increasing the acceleration rate of vehicles and reducing their deceleration rate can reduce congestion and delay, while increasing the capacity of the road network based on the CTM.

Furthermore, the CTM exhibits robust scalability, and innovative methods can be developed based on it. Panda et al. [28] implemented an interactive multimodel filtering model in the CTM framework and used it for traffic density estimation on the urban expressways. Zhou and Wang [29] defined the importance of critical elements in urban transport networks from the perspectives of vulnerability and potential and proposed a new method for identifying these critical elements based on the CTM. Moreover, the CTM is a popular method for simulating and analyzing control strategies for highway traffic flow. Kotsialos and Papageorgiou [30] proposed a design method for controlling strategies for highway network traffic based on the CTM. Li et al. [31] used the CTM to simulate and verify the improvement effects of ramp control and variable speed limit control on freeway congestion management. They also used the CTM to validate and derive the globally optimal solution for controlling strategies on freeways [32].

The CTM emerges as a valuable tool for unveiling traffic phenomena resulting from connected autonomous vehicle (CAV) integration. Jin et al. [33] introduced the variable cell transmission model to analyze mixed traffic flow, comprising human-driven vehicles (HDVs), and CAVs. As CAV market penetration rates rise, traffic capacity increases (up to 1.41 times that of homogeneous HDV flow), and congestion dissipation time decreases by 25%. Yao et al. [34] presented a CTM-based traffic signal timing model for mixed traffic flow with CAVs and HDVs. Optimizing traffic signals with the proposed model reduces congestion range and dissipation time, resulting in an 11.11% increase in average dissipation

efficiency. Furthermore, CAVs significantly reduce traffic delay, with homogeneous CAVs experiencing 14.81% less delay than homogeneous HDV traffic flow. This suggests the potential for CAVs to alleviate congestion and enhance signalized intersection capacity [34]. Wu et al. [27] introduced the CTM for analyzing congestion in mixed traffic flow with CAVs and HDVs. It demonstrates that CAVs substantially alleviate congestion, revealing a positive correlation between bottleneck duration and traffic congestion level. Congestion assessment results show minor variations under different model parameters, but these variations have a negligible impact [27].

This study proposes an improved the CTM called the lane-changing selection cell transmission model (ls-CTM), which alters the selection probability of different downstream cells in the diverging cell flow rule to substitute the driver's lane-changing probability at the prewarning point. The ls-CTM aims to analyze the impact of prewarning distances on upstream traffic flow efficiency and safety at incident points. The space mean speed (SMS) and speed deviation (SD) are employed as evaluation metrics. Among these, SMS is a commonly used indicator for assessing traffic efficiency, while SD has also been applied by researchers [35] to evaluate traffic safety. Simulation experiments are conducted to examine the effects of prewarning distances of 50, 100, and 150 m on SMS and SD as single-lane traffic volume gradually increases from 200 to 1,800 veh/hr. The results show that all three prewarning distances significantly improve the efficiency and safety of the road section under a flow rate of 400–800 veh/hr.

The main contributions of this study are as follows:

(1) The composition of divergent elements in the original CTM has been improved, enabling the improved the CTM, known as ls-CTM, to simulate decision-making in lane-changing behavior of highway traffic flow. This lays the foundation for studying the impact of warning distance on lane-changing probability, which in turn affects road efficiency and safety.

(2) The proposed model is used to analyze the effects of different prewarning distances under different flow conditions on SMS and SD of road sections, providing information on the applicability of these distances under varying flows.

This study proceeds as follows: Section 2 describes the ls-CTM method used in this study and the specific parameters used in the simulation experiments. Section 3 presents the simulation process and results of the three-lane expressway model. Section 4 analyzes and discusses the results and proposes conclusions on the effectiveness and applicability of prewarning distances under different traffic volume conditions. Finally, we summarize the contribution of this study to expressway traffic management and control.

2. Methodology

2.1. Definition of Lane-Changing Selection Behavior under Prewarning. As shown in Figure 1, vehicles generally travel along the lane they are driving on an expressway. In the case of no prewarning, if an incident occurs on a lane, vehicles
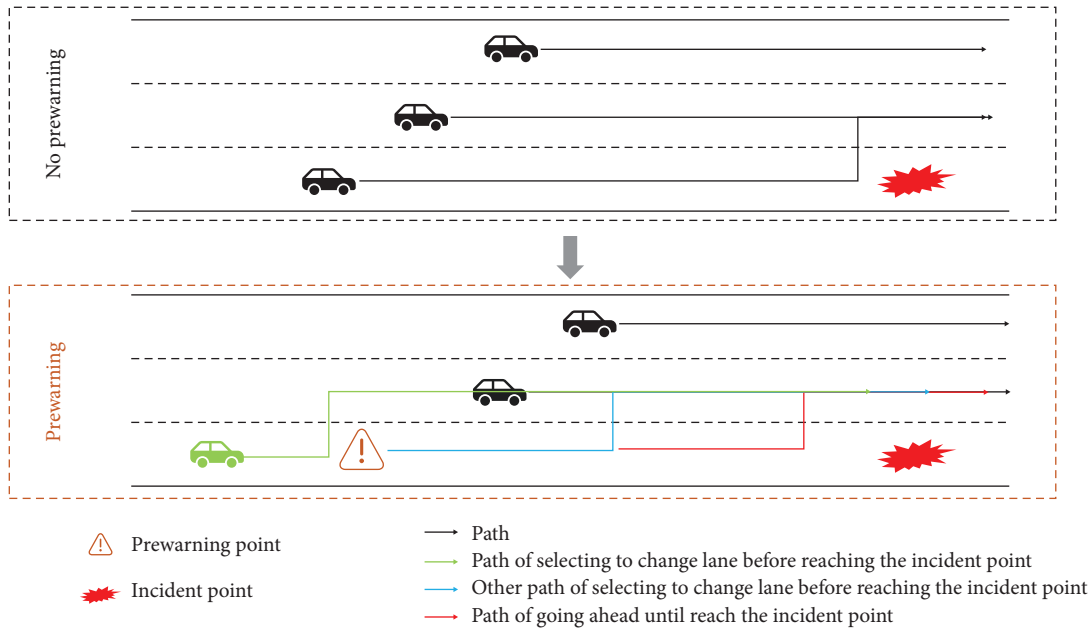
FIGURE 1: A schematic diagram of the definition of lane-changing selection behavior under prewarning.

TABLE 1: Cell types in cell transmission model.

Cell type	Number of incoming connectors	Number of outgoing connectors
Source cell	0	1
Sink cell	1	0
Ordinary cell	1	1
Diverging cell	1	≥ 2
Merging cell	≥ 2	1

will generally discover that the lane ahead is affected by the incident and cannot be used when they are about to reach the accident site. At this point, vehicles are compelled to change lanes and subsequently proceed smoothly to their downstream destination. However, if prewarning information is set up upstream of the incident site, as in the prewarning case shown in Figure 1, some vehicles will choose to change lanes at the prewarning point or continue to move forward. During the process of continuing to move forward, some vehicles will also choose to change lanes before reaching the incident site. Naturally, there are still vehicles that arrive at the incident site before changing lanes.

In the aforementioned scenario, there is a certain probability value for vehicles to change lanes. In the original CTM, the lane-changing behavior of traffic flow is determined by the path, and this behavior is influenced by the judgment rules of diverging type cells. Therefore, in the next section will improve the original CTM so that the diverging cells have the ability to simulate the probability of traffic flow changing lanes.

2.2. Update Rules in Cell Transmission Model. There are five types of cells in the CTM: source, sink, ordinary, diverging, and merging, as shown in Table 1 [10]. The source cell is a cell that provides traffic demand. The sink cell assumes an infinite capacity to receive traffic demand leaving the road network. The number of vehicles staying in the source cell during each time period depends on the demand flow rate, and its update rule is shown in Equation (1). The number of vehicles staying in ordinary, diverging, and merging cells during each time period depends on the upstream inflow and downstream outflow at the previous moment, with the difference being the number of incoming and outgoing connectors. Their update formulas are shown in Equations (2)–(4). The update rule for the sink cell is shown in Equation (5). It is worth emphasizing that the model assumes traffic flow within a cell is homogenous, meaning there are no variations in driving behavior or vehicle sizes.

$$x_i(t) = x_i(t-1) + d_i(t-1) - y_{i,j}(t-1), \tag{1}$$

$$x_i(t) = x_i(t-1) + y_{k,i}(t-1) - y_{i,j}(t-1), \tag{2}$$

$$x_i(t) = x_i(t-1) + y_{k,i}(t-1) - \sum_J y_{i,j}(t-1), \tag{3}$$

$$x_i(t) = x_i(t-1) + \sum_K y_{k,i}(t-1) - y_{i,j}(t-1), \tag{4}$$

$$x_i(t) = x_i(t-1) + y_{k,i}(t-1). \tag{5}$$

All definitions and notations used in the model formulation are summarized in the following:

i—the index of the cell, j—the index of the cell which is downstream of cell i, J—set of all cells downstream of a diverging cell, k—the index of the cell which is upstream of cell i, K—set of all cells immediately upstream of a merging cell, $d_i(t)$—demand from source cell i, $x_i(t)$—cell occupancy of cell i at time t, and $y_{i,j}(t)$—flow from cell i to cell j at time t.

2.3. Flow Rules in Cell Transmission Model

2.3.1. Ordinary Link. The flow of traffic between cells is achieved through connectors, also known as links, between cells. The volume of traffic that an upstream cell intends to transfer downstream is denoted as its sending capacity. The ability of the downstream cell to receive traffic from the upstream cell is called its receiving capacity. The flow rule for a link is to take the minimum value between the sending and receiving capacities. Equations (5)–(7) describe the flow rules for ordinary links as follows:

$$S_i(t) = \min(x_i(t), Q_i), \tag{6}$$

$$R_j(t) = \min\left(Q_j, \frac{w}{v}\left(\rho_{\text{jam}} - x_j(t)\right)\right), \tag{7}$$

$$y_{i,j}(t) = \min\left(S_i(t), R_j(t)\right). \tag{8}$$

All definitions and notations used in the model formulation are summarized in the following:

$S_i(t)$—send capacity of cell i at time t, $R_j(t)$—receive capacity of cell j at time t, Q_i—flow capacity out of cell i, w—speed of shockwave, v—speed of free flow, and ρ_{jam}—jam density.

2.3.2. Merging Link. If the receiving capacity of a merging cell can accommodate all or part of the sending capacity from its upstream cells, then the flow rule for the merging link is the same as that for an ordinary link. However, if the total sending capacity from upstream cells exceeds the receiving capacity of the merging cell, then the amount of flow from each merging link to downstream is determined proportionally based on the maximum sending capacity among the upstream cells, as shown in Equation (8).

$$y_{k,i}(t) = x_{k,i}(t) \times \frac{Q_k}{\sum_K Q_k}. \tag{9}$$

2.4. Lane-Changing Probability in Diverging Link. This study aims to examine the impact of prewarning distance on operational efficiency and traffic safety. It is established that prewarning information can influence the lane-changing behavior of drivers upstream of an incident site. Therefore, this study proposes modifications to the rules for diverging cells in the original CTM.

In this study, diverging cells simulate lane-changing behavior between lanes in traffic networks to model expressway traffic flow, as opposed to the original CTM rule, which determined flow based on the path from the origin to the destination cell downstream. Specifically, we transform the original rule for diverging cells based on path into a probabilistic rule based on whether a vehicle changes lanes or not. The flow in diverging cells is divided into different flows according to the probability of lane changing, as shown in Equation (9). Regardless of which cell is selected for the outflow, the sum of all probabilities must be equal to 1, as shown in Equation (10).

$$x_{i,j}(t) = x_i(t) \times p_{i,j}, \tag{10}$$

$$\sum_J p_{i,j} = 1. \tag{11}$$

All definitions and notations used in the model formulation are summarized in the following:

$x_{i,j}(t)$—determined flow from cell i to cell j at time t and $p_{i,j}$—probability of selecting flow to the downstream cell j in a diverging cell i.

If the sending capacity of a diverging cell can be fully or partially accommodated by its downstream cells, then the flow rule for the diverging link is identical to that for an ordinary link. However, if the total receiving capacity of downstream cells is less than the sending capacity of the diverging cell, then the amount of flow from each diverging link to downstream is determined proportionally according to the ratio between the sending capacity intended for downstream and the total sending capacity, as shown in Equation (11).

$$y_{i,j}(t) = \min\left(x_{i,j}(t), R_j(t)\right) \times \frac{x_{i,j}(t)}{S_i(t)}. \tag{12}$$

Finally, it is imperative to acknowledge that as vehicles draw closer to the incident site, drivers exhibit an increased propensity to perform lane changes. This behavior stems from the fact that refraining from lane changes would result in drivers being confined to the incident site, with lane-changing being the sole means to navigate past the incident site and continue downstream. Consequently, the lane-changing probability can be formally expressed as follows:

$$p_{i,j} = \begin{cases} 1 & \text{if the downstream is the incident site} \\ \dfrac{1}{1 + a \cdot e^{-bl}} & \text{otherwise} \end{cases}. \tag{13}$$

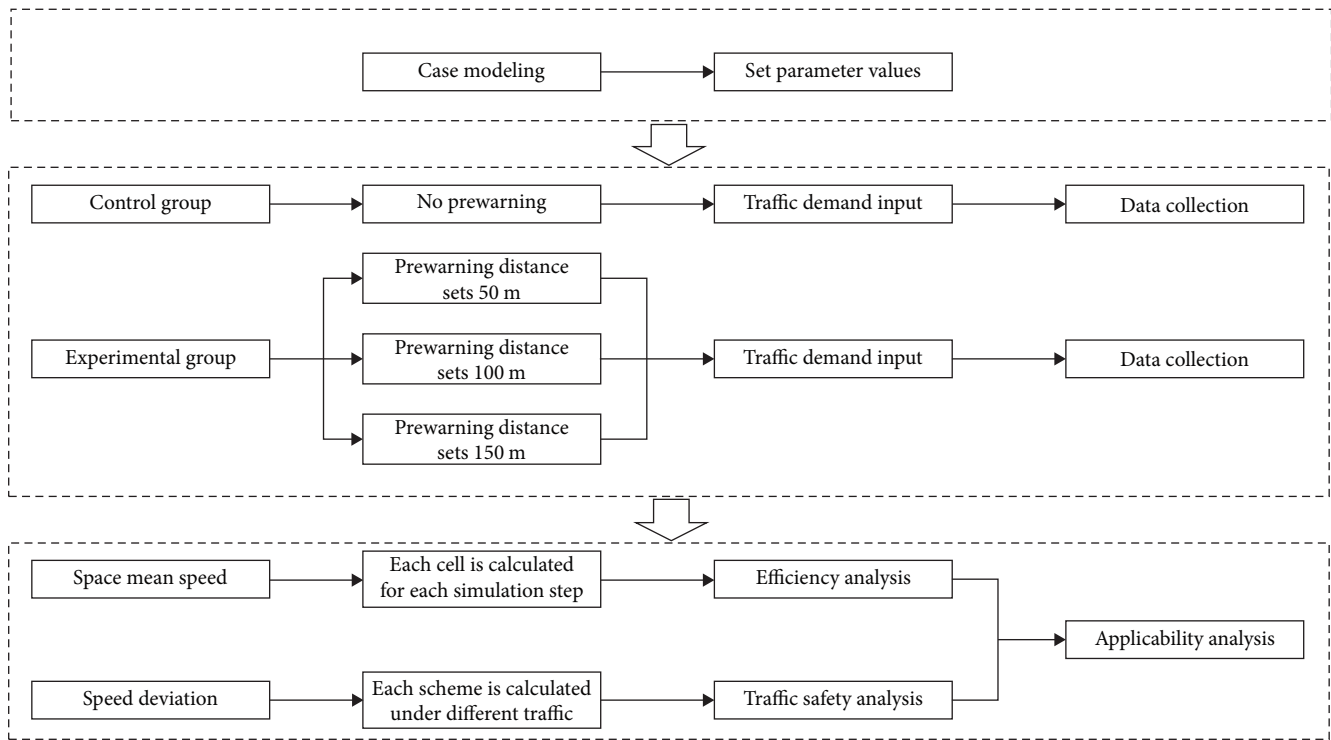All definitions and notations used in the model formulation are summarized in the following:

FIGURE 2: Simulation and analysis flowchart.

a, b—parameters in the lane-changing formula, where both a and b belong to the interval $(0-1)$ and l—distance from the incident site.

Equation (12) represents the probability formula for lane-changing under incident conditions. It is worth noting that the parameter l is technically a negative value since, with the incident site as the origin, lane changes occur upstream, or to the left of the origin. However, for the sake of mathematical consistency, a positive representation of l is used. A larger positive value of l signifies that vehicles are positioned further upstream from the incident site. As l approaches the origin from the left side, the lane-changing probability tends toward 1, as it becomes necessary to change lanes to move downstream. Conversely, as l approaches infinity, the lane-changing probability approaches 0.

3. Case Analysis

3.1. Simulation Description. This experiment examined the impact of prewarning distance on the SMS and SD at the Shanghai Middle Ring Line-Shenjiang Interchange, using the design specifications for this expressway segment as model parameters. The expressway is a three-lane roadway with a design speed of 80 km/hr and a capacity of 1,800 veh/hr. As shown in Figure 2, the simulation and analysis were conducted in three main steps:

Step 1: a simulation model was established based on the case study, with default parameter values derived from the survey data.

Step 2: four groups were established for a simulation experiment: a control group without prewarning, and three

experimental groups with prewarning distances of 50, 100, and 150 m. Traffic demand was gradually increased from 200 up to 1,800 veh/hr in increments of 200 veh/hr, and simulation data were collected for each group.

Step 3: the SMS and SD were selected as evaluation indicators. The collected data were calculated using formulas. The SMS of each cell was calculated in each simulation step. The SD of different schemes was calculated under varying traffic conditions. Results were organized and analyzed for efficiency and safety. Finally, the applicability of different schemes under various traffic conditions was determined based on their combined improvement on efficiency and safety.

The choice of a 50-m prewarning distance aligns precisely with configuration of ls-CTM, with a 25-m cell length and 1-s time step, ensuring numerical stability. Moreover, empirical data, as found in literature [36], confirm that real-world highway driving maintains headways within the 1–3 s range, substantiating the practicality of the chosen prewarning distances. Additionally, human driver reaction times, critical for traffic safety, typically fall between 0.6 and 1 s. A shorter prewarning distance, like 25 m, would risk inadequate driver response time. Conversely, longer distances might compromise precision, impacting real-world applicability. Hence, the 50-m choice strikes a precise balance for meaningful, real-world applicable results.

This experiment used a one-way three-lane cell transmission model to study the impact of prewarning distance on SMS and SD. The program was developed using Python, with a simulation step length of 1 s. Thus, the length of each cell was designed to be 25 m based on the design speed.
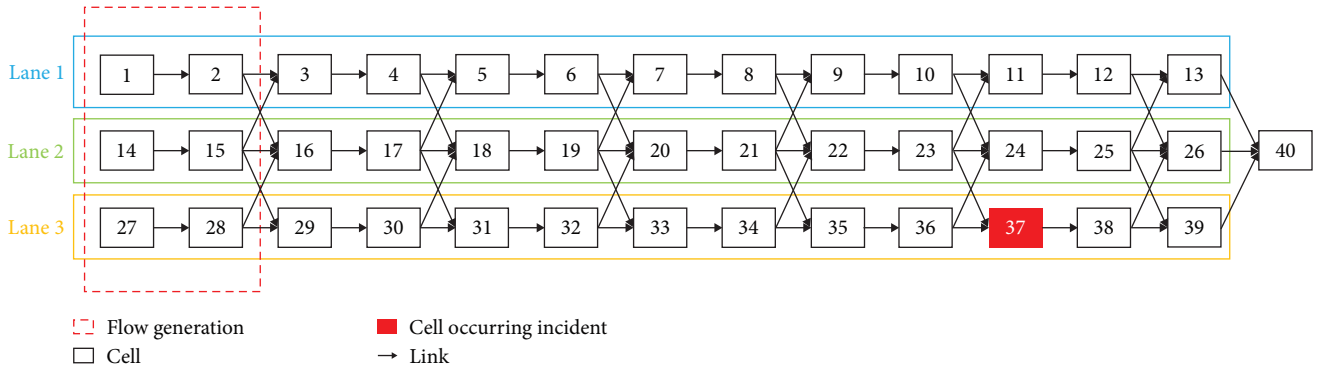
FIGURE 3: Case modeling: cell transmission model of three-lane expressway.

TABLE 2: Parameter matrix of the simulation.

Parameter	Value
Simulation duration (step)	600
Number of cells	40
Length of cells (km)	0.025
Speed of free flow (km/hr)	80
Capacity (veh/hr)	1,800
Jam density (veh/km)	120
Speed of shockwave (km/hr)	18.46

The three-lane cell transmission model used in this experiment is shown in Figure 3, with each lane divided into 13 cells numbered sequentially. Cells 3–13 on Lane 1, cells 16–26 on Lane 2, and cells 29–39 on Lane 3 constituted the segment studied in this experiment. Cells 1, 2, 14, 15, 27, and 28 were used to simulate traffic demand generation and buffer against the target segment. Cell 37 was designated as the location of a simulated incident, with its maximum sending capacity reduced to zero. Cell 40 served as a sink cell, receiving all traffic demand generated in the experiment.

3.2. Simulation Setup. Each simulation has duration of 6 min and contains 600 steps. Based on the proposed model, initial configurations are employed in the simulations so that:

(1) In the first 200 steps, the generated flow rates for all lanes were set to 800 veh/hr in order to achieve the experimental preheating purpose.

(2) In the last 200 steps, the generated flow rates for all lanes were set to 400 veh/hr successively to achieve the goal of demand dissipation.

The simulation uses the following parameters (Table 2):
The specified parameters in the model include a free-flow speed of 80 km/hr, equivalent to ~22.22 m/s, a cell length measuring 25 m, and a time step of 1 s. This configuration ensures that the CFL number [37], computed as the product of the simulation time step and free-flow speed divided by the cell length (CFL = 22.22 × 1/25), remains below 1, thus upholding numerical stability in the CTM.

Based on the video data collected at the Shanghai Middle Ring Line-Shenjiang Interchange, which was subsequently transformed into trajectory data, we estimated the shockwave speed of the experimental road section using the method proposed in reference [38].

The 6-min duration was chosen to study the immediate effects of varying prewarning distances from the incident site. While longer congestion may occur, the focus here was on initial responses and impacts. This duration offered valuable insights into early stage congestion patterns, laying the foundation for future research into longer-term dynamics.

3.3. Model Simulation and Analysis

3.3.1. Efficiency Analysis. SMS [11] refers to the average speed of vehicles over a specific section of a highway or a given spatial area. It is typically calculated by measuring the distance traveled by vehicles within that area and dividing it by the total travel time. SMS provides valuable insights into traffic flow and congestion levels within a particular link, making it a crucial metric for transportation analysis and management.

Figures 4–6 are all composed of 3 by 4 subfigures. The vertical axis of each figure represents the gradually increasing generated flow rate of lanes, and the horizontal axis represents the control group experiments and simulation experiments with prewarning distances of 50, 100, and 150 m, respectively. In each subfigure, the horizontal axis represents the cells of the experimental section.

In the control group experiments of the first column in Figure 4, the generated flow rates are 200, 400, and 600 veh/hr, respectively. It can be observed that in the control group, as the generated flow rate gradually increases, the yellow zone representing SMS reduction gradually expands. However, for the three experimental groups with prewarning, the degree of SMS reduction is lower than that of the control group without prewarning. Nevertheless, after setting the prewarning, the area of SMS reduction increases and extends upstream because vehicles change lanes ahead of time, which interferes with the normal traffic flow.

In the control group experiments of the first column in Figure 5, the generated flow rates are 800, 1,000, and 1,200 veh/hr, respectively. At this point, due to the increase in generated flow rate, the area of SMS reduction caused by incidents has already covered the entire upstream section. However, for the three experimental groups with prewarning,
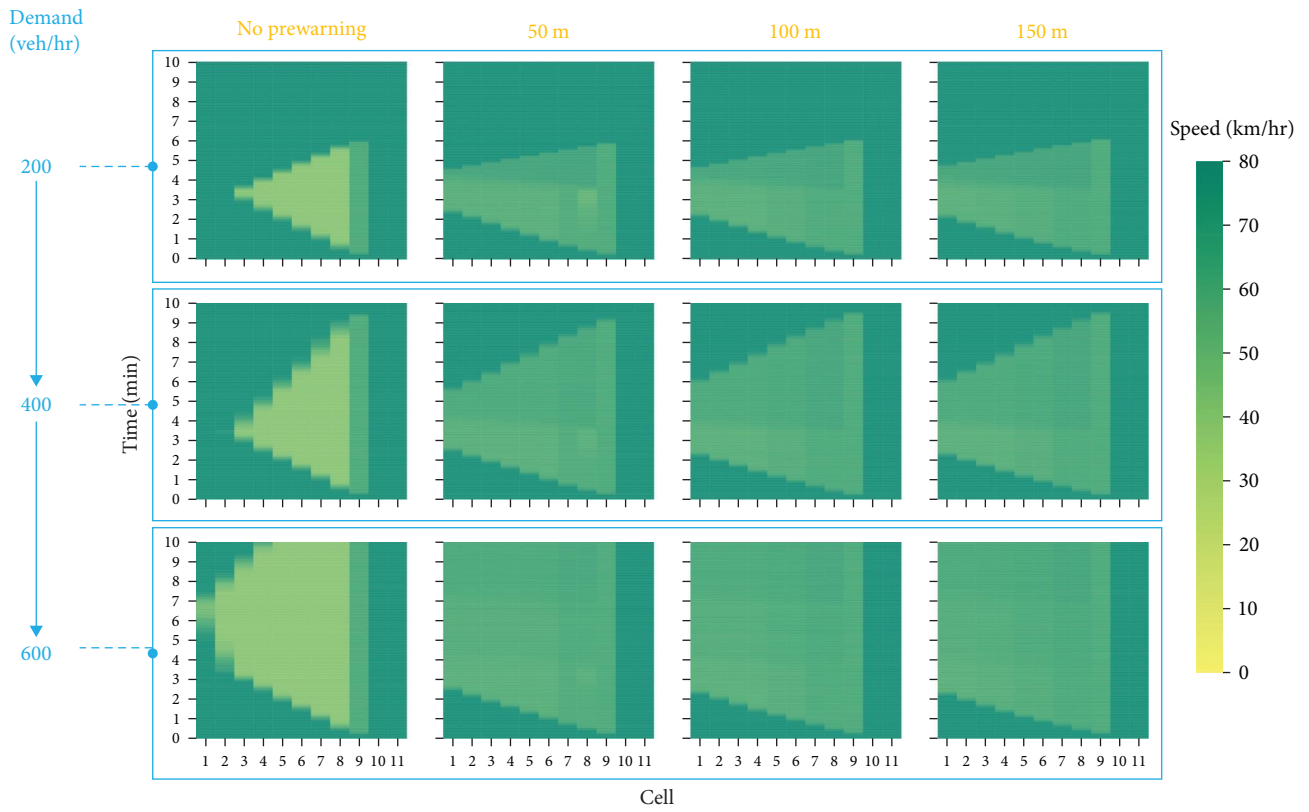
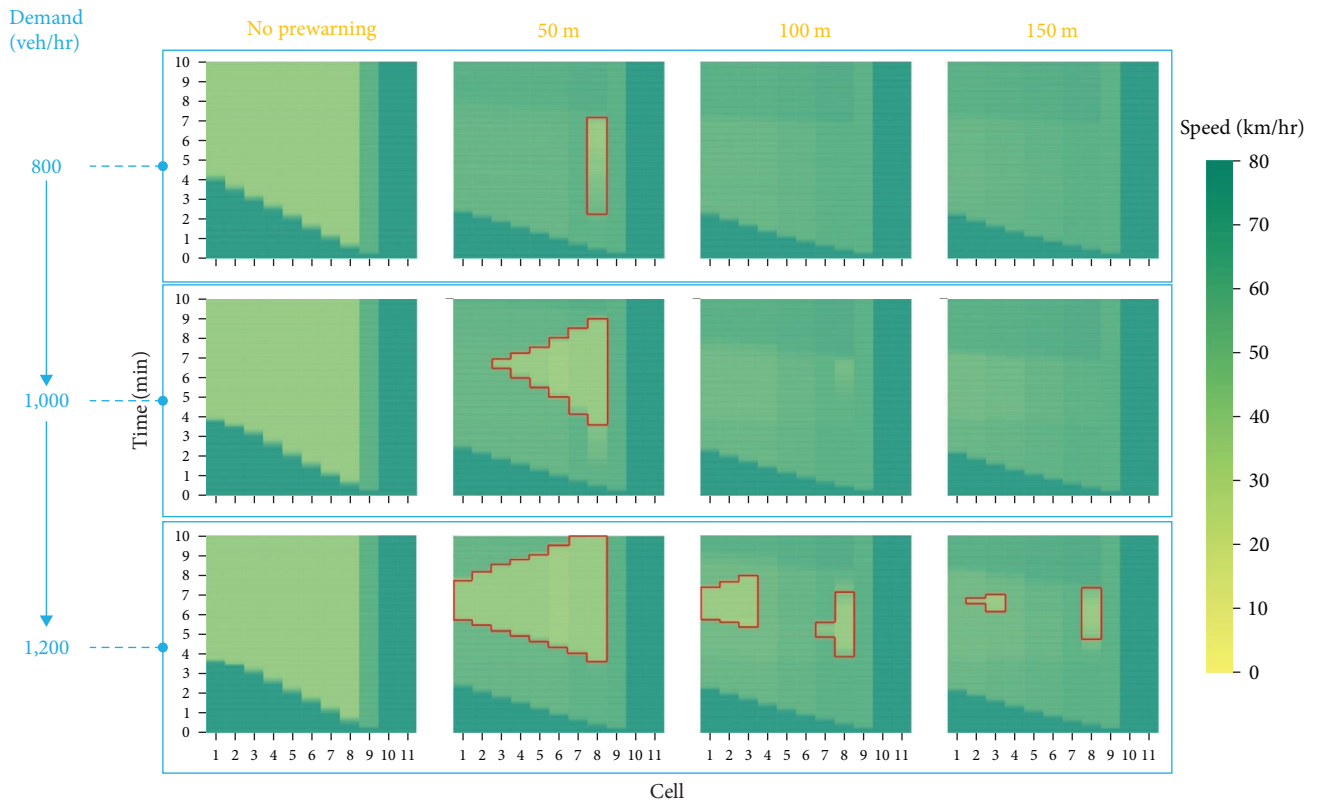FIGURE 4: Heatmap for SMS at different flow Part 1.

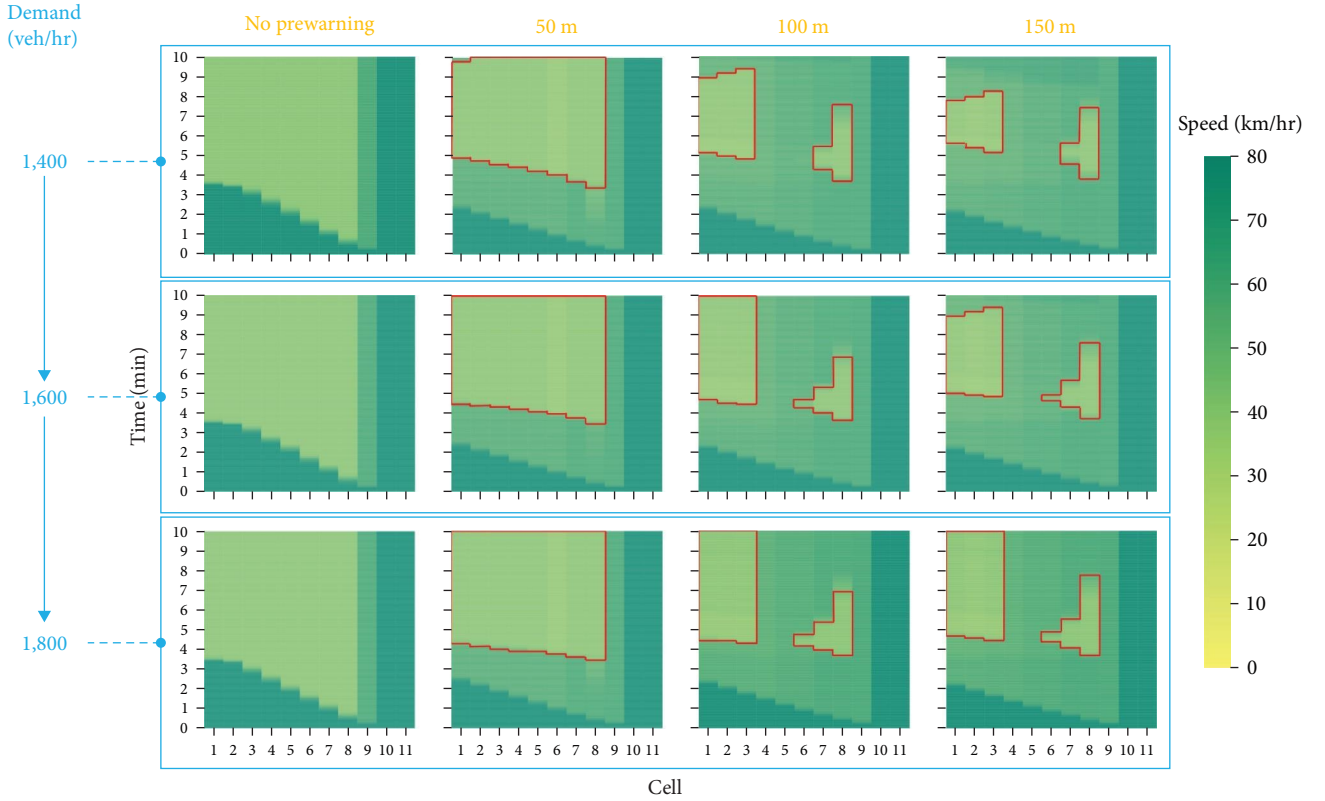FIGURE 5: Heatmap for SMS at different flow Part 2.

FIGURE 6: Heatmap for SMS at different flow Part 3.

the degree of SMS reduction is still lower than that of the control group without prewarning. Because the generated flow rate remains high, the relief effect of the 50-m prewarning distance on SMS reduction has begun to show insufficient relief. This can be demonstrated by the emergence of darker subregions within the complete area of SMS reduction. When the generated flow rate reaches 1,200 veh/hr, even when the prewarning distance is set to 150 m, darker subregions of SMS reduction appear.

In the control group experiments of the first column in Figure 6, the generated flow rates are 1,400, 1,600, and 1,800 veh/hr, respectively. Darker subregions of SMS reduction have already appeared in all experimental groups. For the experimental groups with prewarning distances of 50 and 100 m, the subregion area reaches its maximum when the generated flow rate is 1,600 veh/hr. For the experimental group with a prewarning distance of 150 m, the subregion area reaches its maximum when the generated flow rate is 1,800 veh/hr.

3.3.2. Traffic Safety Analysis. In this study, SD [39] specifically refers to the standard deviation of speed. SD can serve as a quantitative measure to assess the variability in vehicle speeds specifically on expressways. A higher SD value signifies a broader dispersion in vehicle speeds, which correlates with an increased incident rate on the expressway. Conversely, a lower SD value indicates a more uniform and consistent speed distribution among vehicles, concomitant with

a decreased incident rate of traffic flow on the expressway. Given this contextual understanding, we have employed SD as a primary quantitative metric within this research paper. It serves as a robust tool for a comprehensive evaluation of traffic safety and a detailed exploration of the effects of the three measures on improving safety conditions. The calculation method of SD is as follows:

$$SD = \sqrt{\frac{\sum_{n=1}^{N}(v_n - \overline{v})^2}{N - 1}}, \tag{14}$$

All definitions and notations used in the model formulation are summarized in the following:

n—index of cells, v_n—space mean speed of the cell n, and $\overline{v}$—space mean speed of experimental segment.

Table 3 displays the results of SD for the three measures with prewarning distances of 50, 100, and 150 m. The value of 0 for prewarning distance represents no prewarning measure. The results indicate that the SD values of the measures with prewarning are lower than those without a prewarning measure. Overall, the farther the prewarning distance are, the lower the SD value is. When the flow rate is between 200 and 600 veh/hr, the differences in SD values between the three measures are small. Starting from a flow rate of 800 veh/hr, the difference in SD values between the measure with a 50 m prewarning distance and the other two measures begins to increase. Starting from a flow rate of 1,200 veh/hr, the difference in SD values between the measure with a 100-m

TABLE 3: SD value at different flow and prewarning distance.

Flow (veh/hr)	Prewarning distance (m)			
	0	50	100	150
200	13.8814	9.1464	8.8194	8.6678
400	16.1221	9.4733	9.1172	8.9067
600	18.0352	8.8832	8.553	8.36
800	18.0341	10.0661	8.9644	8.721
1,000	18.0429	12.949	9.4327	9.1478
1,200	18.0405	15.2116	11.7358	10.1989
1,400	18.0276	16.3528	13.086	12.2097
1,600	18.0484	16.4968	13.7166	13.2346
1,800	17.9656	16.6299	13.9283	13.8034

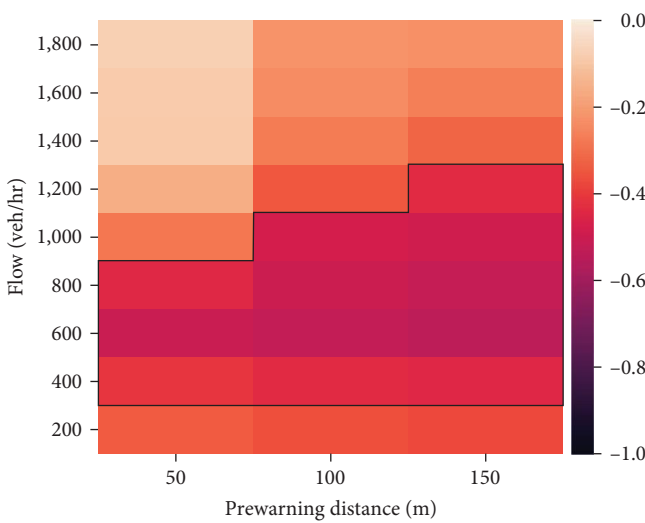FIGURE 8: Applicability analysis of prewarning distance under different traffic flow.

FIGURE 7: Comparison of different prewarning distances in reducing the degree of SD compared to the control group with no prewarning.

prewarning distance and the measure with a 150-m prewarning distance begins to increase. However, when the flow rate reaches 1,800 veh/hr, the difference between the two measures decreases again.

Figure 7 presents a comparison of different prewarning distances in reducing the degree of SD, using the SD values of the control group without prewarning as a reference. The results indicate that the three measures significantly reduce the SD value when the flow rate is between 400 and 800 veh/hr. When the flow rate reaches 1,000 veh/hr, the measures with prewarning distances of 100 and 150 m significantly reduce the SD value. When the flow rate is 1,200 veh/hr, the measure with a prewarning distance of 150 m significantly reduces the SD value, indicating an improvement in traffic safety.

4. Discussion

The simulation experiment results show that the three measures have different degrees of relief on SMS reduction under different flow conditions, but all perform better than taking no measures in improving traffic safety. Specifically, when
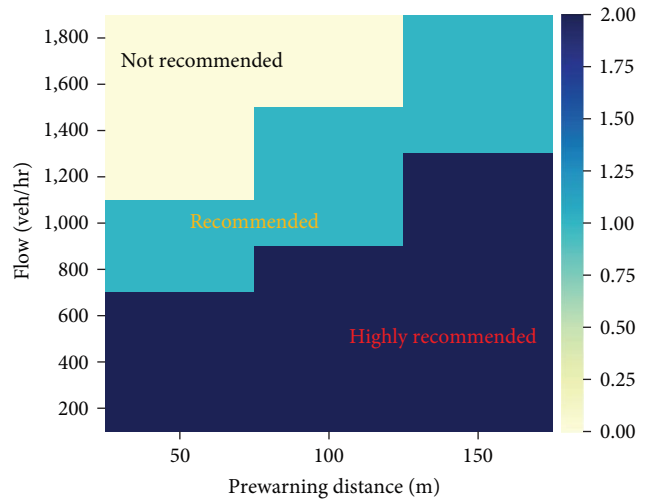
the prewarning distance is set at 50 m, it can alleviate the degree of SMS reduction for the entire section when the flow rate is between 200 and 800 veh/hr. After the flow rate exceeds 800 veh/hr, the relief ability of this measure gradually decreases. When the prewarning distance is set at 100 m, it can alleviate the degree of speed reduction for the entire section when the flow rate is between 200 and 1000 veh/hr. After the flow rate exceeds 1,000 veh/hr, the relief ability of this measure gradually decreases. When the prewarning distance is set at 150 m, it can alleviate the degree of SMS reduction for the entire section when the flow rate is between 200 and 1,200 veh/hr. After the flow rate exceeds 1,200 veh/hr, the relief ability of this measure gradually decreases. This phenomenon of decreasing relief effect is since traffic flow begins to change lanes and divert at the prewarning, resulting in new bottlenecks. As the flow rate gradually increases, this bottleneck becomes more and more evident.

In terms of improving traffic safety performance, the effects of the three measures are significant when the flow rate is between 400 and 800 veh/hr. As the flow rate increases, the farther the prewarning distance is, the greater the improvement effect on traffic safety, which approaches the maximum. This phenomenon occurs because when the flow rate is low, changing lanes closer to the incident site is more likely to disrupt normal vehicle speeds. Prewarning makes drivers more prepared to change lanes in an orderly manner, which improves traffic safety. However, such an orderly improvement has limited capabilities in improving traffic safety. As a result, the safety improvement effect approaches its limit after the flow rate reaches 1,400 veh/hr.

As shown in Figure 8, based on the performance of the three measures in alleviating SMS reduction and reducing SD under different flow rates, this study summarizes the applicability ranges of the three measures as follows:

(1) Prewarning distance of 50 m: recommended for use when the flow rate is between 200 and 600 veh/hr; can be used when the flow rate is between 800 and

1,000 veh/hr; not recommended for use when the flow rate is between 1,200 and 1,800 veh/hr.

(2) Prewarning distance of 100 m: recommended for use when the flow rate is between 200 and 800 veh/hr; can be used when the flow rate is between 1,000 and 1,400 veh/hr; not recommended for use when the flow rate is between 1,600 and 1,800 veh/hr.

(3) Prewarning distance of 150 m: recommended for use when the flow rate is between 200 and 1,200 veh/hr; can be used when the flow rate is between 1,400 and 1,800 veh/hr.

5. Conclusions

The proposed ls-CTM can be used for expressway scenarios to divide traffic flow and analyze the effect of lane-changing prewarning distances on improving the operational quality and safety. Simulation results show that implementing pre-warning distances of 50, 100, or 150 m can effectively alleviate traffic congestion and improve traffic safety under various traffic demands. This provides guidance for traffic management and decision-making in expressway scenarios. It does this by analyzing the applicability ranges of these measures, which can be summarized in the following three points:

(1) The ls-CTM proposed in this study can be used to divide the traffic flow in a cell into different flows heading toward different downstream cells, which is suitable for expressway scenarios that require probabilistic lane-changing decisions.

(2) In the case of the Shenjiang Interchange three-lane expressway, this study employed a controlled variable method. This method was used to establish a control group without prewarning and three experimental groups with different prewarning distances. Subsequently, simulation analyses were conducted under varying traffic demands. The results show that under low traffic demand (200–600 veh/hr), the three measures of prewarning distances of 50, 100, and 150 m have significant effects on alleviating traffic congestion upstream of the incident site and promoting traffic safety. As the demand increases to 800, 1,000, and 1,400 veh/hr, the efficiency-promoting effects of the prewarning distances of 50, 100, and 150 m begin to decrease, respectively. However, regardless of whether the distance of the prewarning is small or large, it has a positive effect on traffic safety.

(3) This study provides an analysis of the applicability ranges of prewarning distances for improving traffic safety and alleviating SMS reduction under different flow rates. The simulation results suggest that implementing prewarning distances of 50, 100, or 150 m can be effective in various scenarios, with recommended usage ranges varying based on the flow rate. This analysis can provide guidance for traffic management and decision-making in expressway scenarios to improve the operational quality and safety.

The ls-CTM proposed in this study assumes that the vehicles in the cell are homogeneous and does not consider the proportion of different vehicle types. Therefore, based on the mixed traffic flow fundamental diagram, the ls-CTM can be improved to consider the inherent structural impact of large vehicles on traffic flow. At the same time, the lane-changing probability selected in the ls-CTM proposed in this study is constant and does not consider drivers' perception of the distance to the incident site or individual driving behavior preferences of drivers. Therefore, traffic flow in each cell can be further divided into different flows corresponding to the different driving behavior preferences, using the corresponding lane-changing probability function.

Data Availability

All the data used to support the findings of this study are included within the study.

Conflicts of Interest

The authors declare that they have no conflicts of interest.

Acknowledgments

References

[1] C. Systematics, *An Initial Assessment of Freight Bottlenecks on Highways*, Create Space Independent Publishing Platform, 2005.

[2] J. A. Lindley, "The urban freeway congestion problem," *Transportation Research Circular*, vol. 344, 1989.

[3] A. Skabardonis, K. Petty, P. Varaiya, and R. Bertini, *Evaluation of the freeway service patrol (FSP) in Los Angeles*, California Path Program Institute of Transportation Studies University of California, Berkeley, 1998.

[4] J. He, Z. He, B. Fan, and Y. Chen, "Optimal location of lane-changing warning point in a two-lane road considering different traffic flows," *Physica A: Statistical Mechanics and Its Applications*, vol. 540, Article ID 123000, 2020.

[5] K. Nagel and M. Schreckenberg, "A cellular automaton model for freeway traffic," *Journal de Physique I*, vol. 2, no. 12, pp. 2221–2229, 1992.

[6] J. Wang, S. Li, Y. Lu, and L. Wang, "A division method of determining the early-warning zone on an expressway for automated vehicles," *Discrete Dynamics in Nature and Society*, vol. 2020, Article ID 6689089, 10 pages, 2020.

[7] X. Tan, Q. Deng, and X. Hu, "Research on vehicle carrying efficiency of three-lane expressway based on DEA method," *Transportation Letters*, vol. 14, no. 8, pp. 838–848, 2022.

[8] F. Storani, R. Di Pace, F. Bruno, and C. Fiori, "Analysis and comparison of traffic flow models: a new hybrid traffic flow model vs benchmark models," *European Transport Research Review*, vol. 13, no. 1, pp. 1–16, 2021.

[9] C. F. Daganzo, "The cell transmission model: a dynamic representation of highway traffic consistent with the

hydrodynamic theory," *Transportation Research Part B: Methodological*, vol. 28, no. 4, pp. 269–287, 1994.

[10] C. F. Daganzo, "The cell transformation model, Part II: network traffic," *Transportation Research Part B: Methodological*, vol. 29, no. 2, pp. 79–93, 1995.

[11] M. J. Lighthill and G. B. Whitham, "On kinematic waves II. A theory of traffic flow on long crowded roads," *Proceedings of the Royal Society of London. Series A. Mathematical and Physical Sciences*, vol. 229, no. 1178, pp. 317–345, 1955.

[12] S. Lee, *A Cell Transmission Based Assignment-simulation Model for Integrated Freeway/surface Street Systems*, The Ohio State University, 1996, http://rave.ohiolink.edu/etdc/view?acc_num=osu1103731343.

[13] S. T. Waller and A. K. Ziliaskopoulos, "Stochastic dynamic network design problem," *Transportation Research Record*, vol. 1771, no. 1, pp. 106–113, 2001.

[14] S. T. Waller, K. C. Mouskos, D. Kamaryiannis, and A. K. Ziliaskopoulos, "A linear model for the continuous network design problem," *Computer-Aided Civil and Infrastructure Engineering*, vol. 21, no. 5, pp. 334–345, 2006.

[15] A. Karoonsoontawong and S. T. Waller, "Integrated network capacity expansion and traffic signal optimization problem: robust bi-level dynamic formulation," *Networks and Spatial Economics*, vol. 10, no. 4, pp. 525–550, 2010.

[16] A. K. Ziliaskopoulos, "A linear programming model for the single destination system optimum dynamic traffic assignment problem," *Transportation Science*, vol. 34, no. 1, pp. 37–49, 2000.

[17] K. Doan and S. V. Ukkusuri, "On the holding-back problem in the cell transmission based dynamic traffic assignment models," *Transportation Research Part B: Methodological*, vol. 46, no. 9, pp. 1218–1238, 2012.

[18] Y. Nie, "A cell-based Merchant–Nemhauser model for the system optimum dynamic traffic assignment problem," *Transportation Research Part B: Methodological*, vol. 45, no. 2, pp. 329–342, 2011.

[19] H. Zheng and Y.-C. Chiu, "A network flow algorithm for the cell-based single-destination system optimal dynamic traffic assignment problem," *Transportation Science*, vol. 45, no. 1, pp. 121–137, 2010.

[20] K. Doan and S. V. Ukkusuri, "Dynamic system optimal model for multi-OD traffic networks with an advanced spatial queuing model," *Transportation Research Part C: Emerging Technologies*, vol. 51, pp. 41–65, 2015.

[21] T. Islam, H. L. Vu, N. H. Hoang, and A. Cricenti, "A linear bus rapid transit with transit signal priority formulation," *Transportation Research Part E: Logistics and Transportation Review*, vol. 114, pp. 163–184, 2018.

[22] A. Sumalee, R. X. Zhong, T. L. Pan, and W. Y. Szeto, "Stochastic cell transmission model (SCTM): a stochastic dynamic traffic model for traffic state surveillance and assignment," *Transportation Research Part B: Methodological*, vol. 45, no. 3, pp. 507–533, 2011.

[23] K. Tiaprasert, Y. Zhang, C. Aswakul, J. Jiao, and X. Ye, "Closed-form multiclass cell transmission model enhanced with overtaking, lane-changing, and first-in first-out properties," *Transportation Research Part C: Emerging Technologies Article*, vol. 85, pp. 86–110, 2017.

[24] C. Shirke, A. Bhaskar, and E. Chung, "Macroscopic modelling of arterial traffic: an extension to the cell transmission model," *Transportation Research Part C: Emerging Technologies Article*, vol. 105, pp. 54–80, 2019.

[25] C. Ng, S. Susilawati, M. A. Samad Kamal, and I. M. Leng Chew, "Development of macroscopic cell-dased logistic lane change

[26] H. Xiao, Q. Zhang, S. Ouyang, and A. T. Chronopoulos, "Connectivity probability analysis for VANET freeway traffic using a cell transmission model," *IEEE Systems Journal*, vol. 15, no. 2, pp. 1815–1824, 2020.

[27] Y. Wu, Y. Lin, R. Hu, Z. Wang, B. Zhao, and Z. Yao, "Modeling and simulation of traffic congestion for mixed traffic flow with connected automated vehicles: a cell transmission model approach," *Journal of Advanced Transportation*, vol. 2022, Article ID 8348726, 20 pages, 2022.

[28] M. Panda, D. Ngoduy, and H. L. Vu, "Multiple model stochastic filtering for traffic density estimation on urban arterials," *Transportation Research Part B: Methodological*, vol. 126, pp. 280–306, 2019.

[29] Y. Zhou and J. Wang, "Critical link analysis for urban transportation systems," *IEEE Transactions on Intelligent Transportation Systems*, vol. 19, no. 2, pp. 402–415, 2017.

[30] A. Kotsialos and M. Papageorgiou, "Motorway network traffic control systems," *European Journal of Operational Research*, vol. 152, no. 2, pp. 321–333, 2004.

[31] Y. Li, A. H. F. Chow, and D. L. Cassel, "Optimal control of motorways by ramp metering, variable speed limits, and hard-shoulder running," *Transportation Research Record*, vol. 2470, no. 1, pp. 122–130, 2014.

[32] Y. Li, A. H. F. Chow, and R. Zhong, "Control strategies for dynamic motorway traffic subject to flow uncertainties," *Transportmetrica B: Transport Dynamics*, vol. 7, no. 1, pp. 559–575, 2019.

[33] Y. Jin, Z. Yao, J. Han, L. Hu, and Y. Jiang, "Variable cell transmission model for mixed traffic flow with connected automated vehicles and human-driven vehicles," *Journal of Advanced Transportation*, vol. 2022, Article ID 6342857, 15 pages, 2022.

[34] Z. Yao, Y. Jin, H. Jiang, L. Hu, and Y. Jiang, "CTM-based traffic signal optimization of mixed traffic flow with connected automated vehicles and human-driven vehicles," *Physica A: Statistical Mechanics and its Applications*, vol. 603, Article ID 127708, 2022.

[35] H. Ding, L. Zhang, J. Chen, X. Zheng, H. Pan, and W. Zhang, "MPC-based dynamic speed control of CAVs in multiple sections upstream of the bottleneck area within a mixed vehicular environment," *Physica A: Statistical Mechanics and its Applications*, vol. 613, Article ID 128542, 2023.

[36] L. Li, X. Chen, and Z. Li, "Asymmetric stochastic Tau theory in car-following," *Transportation Research Part F: Traffic Psychology and Behaviour*, vol. 18, pp. 21–33, 2013.

[37] R. Courant, K. Friedrichs, and H. Lewy, "Über die partiellen differenzengleichungen der mathematischen physik," *Mathematische Annalen*, vol. 100, no. 1, pp. 32–74, 1928.

[38] T. Seo, Y. Kawasaki, T. Kusakabe, and Y. Asakura, "Fundamental diagram estimation by using trajectories of probe vehicles," *Transportation Research Part B: Methodological*, vol. 122, pp. 40–56, 2019.

[39] D. H. Solomon, "Accidents on main rural highways: related to speed, driver, and vehicle," US Department of Transportation, Federal Highway Administration, 1974.